Superconductivity: General Theory & Materials Overview
Phys 617, Texas A&M University, April, 2017

1. London equation, London penetration depth: The London theory (due to F. and H. London) omits coherence phenomena such as described in section 5 below, but the theory provides a straightforward picture of magnetic flux exclusion as observed in superconductors, and the London penetration depth (λ) is one of the standard parameters used to characterize the properties of different superconductors. The theory starts with two basic assumptions about superconducting behavior: electron acceleration without resistance, and zero internal *B* field (the experimental *Meissner effect*). From the first assumption, $\frac{d\vec{v}}{dt} = -\frac{e}{m}\vec{E}$ so that

$$\frac{d\vec{j}}{dt} = \frac{ne^2}{m}\vec{E}. \qquad [1]$$

Taking the curl of both sides of [1], and using Faraday's law ($\vec{\nabla}\times\vec{E} = -\frac{1}{c}\frac{\partial\vec{B}}{dt}$), yields

$$\frac{d}{dt}\left(\vec{\nabla}\times\vec{j} + \frac{ne^2}{mc}B\right) = 0. \qquad [2]$$

The Londons noted that setting the expression in parentheses in [2] equal to *zero* rather than simply constant vs. time is consistent with the experimental observation of vanishing magnetic fields in superconductors. This yields one version of the London equation:

$$\vec{\nabla}\times\vec{j} = -\frac{ne^2}{mc}B \equiv -\frac{c}{4\pi\lambda^2}B, \qquad [3]$$

where in the last part $\lambda = \sqrt{mc^2/4\pi ne}$ defines the London penetration depth λ. [Note the text uses Λ; here I use the lower case λ since this is the much more commonly used notation.]

A second expression equivalent to [3] is:

$$\vec{\nabla}\times\vec{\nabla}\times\vec{B} = -\frac{1}{\lambda^2}\vec{B}, \qquad [4]$$

obtained from [3] via Ampere's law ($\vec{\nabla}\times\vec{B} = \frac{4\pi}{c}\vec{j}$). [3] and [4] can be used to show that both *B* and *j* vanish in the interior of a superconductor: from vector calculus the double curl in [4] is $-\nabla^2\vec{B} + \vec{\nabla}(\vec{\nabla}\cdot\vec{B})$, in which the second half vanishes identically from Gauss' law. Therefore,

$$\nabla^2\vec{B} = \vec{B}/\lambda^2, \qquad [5]$$

with the solution (near a flat surface) that *B* decays exponentially, $B = B_{ext}e^{-x/\lambda}$. From [3] this also implies that when *B* decays in a thin surface region, there is also a current density *j* decaying exponentially, screening the interior from the external field. The vanishing of *B* is the Meissner (or Meissner-Ochsenfeld) effect.

2. Interactions between electron pairs: Superconductivity was explained by the BCS theory (Bardeen, Cooper, Schrieffer, 1957), due to pairing of electrons, via an attractive interaction mediated by phonons. As an approximate way to understand this, we consider the simplest form of electron screening corresponding to a dielectric function [same as (17.51) in the text]:

$$\varepsilon(q) = 1 + k_o^2/q^2 \qquad [6]$$

where k_o depends on the electron density. A negative charge $-Q$ in a metal with such a dielectric function is surrounded by an effective potential $(-Q/r)\exp(-k_o r)$; see results following (17.51) in the text. The exponential decay is the result of a region of positive charge due to electrons avoiding the negative charge. Electon-electron interactions are reduced (but not reversed) by such an effect. Including displacements of the positive ions leads to a modification as outlined in chapter 26, which we did not cover but which is quoted here. For classical undamped harmonic oscillators of charge Q the displacement in response to a field $\vec{E}\cos\omega t$ is

$$\vec{u}\cos\omega t = \frac{-Q\vec{E}\cos\omega t}{M(\omega^2 - \omega_o^2)}, \qquad [7]$$

where the natural frequency of the oscillator is $\omega_o = \sqrt{\kappa/M}$. At low frequencies the displacement points along the force, but at frequencies higher than ω_o there is a 180° phase shift. For phonon modes we replace ω_o by the phonon frequency, ω_q, and hereafter we neglect this small frequency entirely, since electrons move much faster than the ions. The resulting ion-charge displacements lead to a dielectric function which can be shown to be [text (26.19)],

$$\varepsilon(q) = 1 - \Omega^2/\omega^2. \qquad [8]$$

The cutoff frequency Ω is the ionic plasma frequency; see more details in chapter 26. The final terms in [6] and [8] are proportional to the electrical susceptibility, and can be added to give

$$\varepsilon(q) = 1 + k_o^2/q^2 - \Omega^2/\omega^2. \qquad [9]$$

This approximate result may be negative for a range of frequencies and wavevectors, and a negative sign changes the electron-electron interaction from repulsive to attractive.

In high-T_c superconductors such as $YBa_2Cu_3O_{7-x}$, there is now a near-consensus that pairing is due to *magnetic* excitations rather than phonon excitations. Changing the oxygen concentration (O_{7-x}) changes the materials from magnetic to superconducting, and the nearness of the superconducting and magnetic states in these materials, as well as the large T_c lends credence to proposals that the pairing in these materials is magnetic excitations, although working out the specifics of this pairing interactions has proved difficult.

For the traditional superconductors with phonon pairing, the *isotope effect* was an early clue that this was indeed the case. The isotope effect is a small change in T_c caused by a change in isotope mass; ideally T_c is proportional to $M^{-1/2}$, where M is the isotope mass, and in many cases that is very close to what is observed. The T_c change is small and careful sample preparation is required to assure that the effect is not dwarfed by other sample-dependent changes. The M dependence arises through connection to the Debye frequency (see equation [11] below); ω_D is related to the speed of sound and the speed of sound is proportional to $\sqrt{K/M}$.

3. BCS ground state, Cooper pairs, coherence length: The phonon-mediated interaction between electrons leads to an effective interaction potential that is weakly attractive for ordinary superconductors. Normally a very weak attractive interaction may not be enough to bind two particles. However, Cooper showed how two electrons could interact in the presence of a filled Fermi sea to form a wavefunction with lower energy than that of two electrons which do not interact. For simplicity, he took the interaction between electrons (with wavevector q) to be constant (V), up to a cutoff energy, taken to be $\hbar\omega_D$, which is the highest phonon energy in the Debye model (since phonons cause the weak attraction). Also, the Fermi surface was assumed spherical. With these simplifications he found a ground-state 2-electron wavefunction,

$$\Psi(\vec{r}_1,\vec{r}_2) \propto \sum_{k>k_F} \psi_{k\sigma}(\vec{r}_1)\psi_{-k,-\sigma}(\vec{r}_2)\frac{V}{(2\varepsilon_k - 2\varepsilon_F)}. \qquad [10]$$

This is a superposition of electron states across the Fermi surface (±*k*), with opposite spin. (*V* is the Fourier transform of the potential, units energy*volume.) The energy, correct for small *V*, is

$$E = 2\varepsilon_F - 2\hbar\omega_D e^{-2/g(\varepsilon_F)V}. \qquad [11]$$

In this solution there is no minimum value of *V* required to obtain a bound state, as long as *V* is attractive. (In contrast, a quantum particle in a square well does have a minimum depth below which there are no bound states.) Hence, *V* need only be positive, and even the weak phonon-mediated attraction can be enough to drive an electronic phase transition. Finally, to be correct for Fermions, each product wavefunction in [10] must be rewritten as an antisymmetrized product rather than a simple product of up and down spin states.

A Cooper pair is a superposition of many plane-wave states, ordinarily in an *s*-state (all phases in [10] identical). The size of the pairs generally agrees with a Heisenberg uncertainty argument; weak *V* implies Ψ which has a large extent relative to the atomic scale. For "low-T_c's" the size is about 10000 Å. This size also defined as the coherence length, denoted ξ_o (these quantities are equivalent in the low-T limit). Together, ξ_o plus the London penetration depth, λ (equation [3]) are the two important length scales for the description of superconductivity.

The BCS ground-state wavefunction is made by filling the metal with pairs. It can be written as a product state:

$$\Psi = A\Psi(\vec{r}_1,\vec{r}_2)\Psi(\vec{r}_3,\vec{r}_4)\Psi(\vec{r}_5,\vec{r}_6)\ldots. \qquad [12]$$

where each of the pair wavefunctions in the product is identical. [More properly, the pair states can be either occupied or unoccupied, with appropriate coefficients. This is typically set out via second quantization—see for example deGennes' text for a nicely written description.] The pair wavefunctions in this product are assumed not to be antisymmetrized; the operator *A* does this for the whole wavefunction--it makes the state a Slater determinant. *A* thus assures that the wavefunction is properly antisymmetric as for Fermions, however, the pairs themselves are identical and obey Bose-Einstein statistics. Fermions thus can act like Bosons, with the BCS ground state regarded as a Bose-condensed fluid of identical pairs. If the magnitude of the attractive interaction between electrons were to increase, the ground state would change from a BCS-like state to one characterized by isolated electron-pair "molecules"; this is the regime of Bose condensation in cooled atomic gases. The BCS regime is in the opposite extreme, with pair wavefunctions extended in space such that the pairs themselves are heavily overlapping.

For high-T_c superconductors the pair wavefunction is considerably smaller than the 10000 Å figure quoted above for simple metals; a representative value is ξ_o = 20 Å. There is also accumulated evidence showing that the pairing wavefunction is more closely *d*-wave in high-T_c superconductors, rather than the *s*-state of the BCS theory.

4. Energy gap: With electrons paired as in [12], excitations from the ground state require breaking pairs. There is an energy gap, $E_g \equiv 2\Delta$, for such excitations due to the bound-state pairing energy. In the BCS theory, Δ is the energy difference appearing as the last term in [11]. The resulting density of states for allowed excitations is sketched below, showing how the single-particle states effectively "pile up" on the two sides of the gap. The functional form in BCS theory is $g(\varepsilon) \propto |E| \Big/ \sqrt{E^2 - \Delta^2}$. On the right is a figure from a tunneling measurement (STM), which is one way for the gap to be seen directly. The superconducting transition temperature (T_c) is related to Δ in the BCS theory according to:

$$2\Delta = 3.53\, k_B T_c. \qquad [13]$$

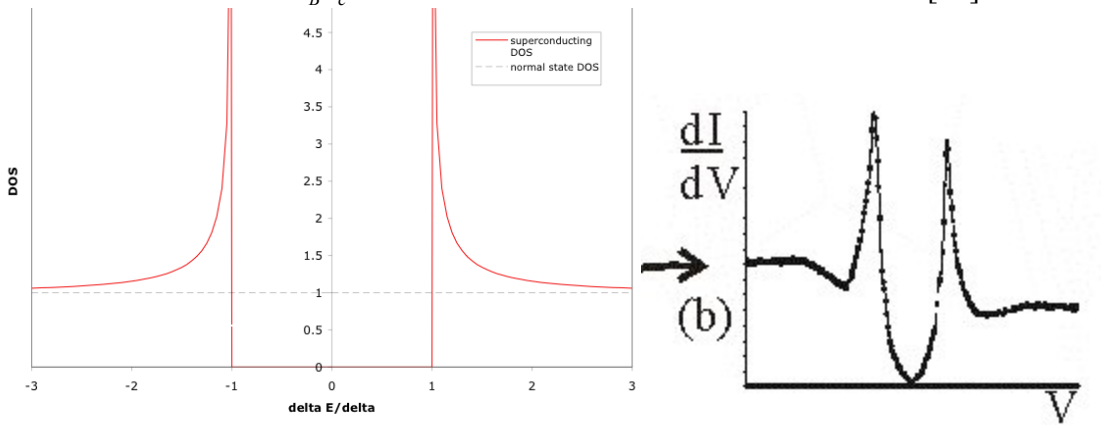

5. Ginzburg-Landau theory. In this model, the superconducting state is characterized by an "order parameter" $\psi(r)$. $\psi(r)$ is a pseudowavefunction: it plays a role much like a wavefunction, but it includes no microscopic features (think of taking a Bloch-type wavefunction but smearing out all the atomic-scale details). For superconductors, $\psi(r)$ can be regarded as having locally the phase of the condensate wavefunction from microscopic theory [12], and an amplitude such that $|\psi(r)|^2 = n_s$, the density of superconducting electrons.

Ginzburg-Landau theory is valid for slowly varying fields, and its accuracy is best for small $\psi(r)$ (a situation occurring near T_c). One of the basic relations is for the electric current density, obtained assuming $|\psi(r)|^2$ is a constant:

$$\vec{J}_{el} = -\left[\frac{2e^2}{mc}\vec{A} + \frac{e\hbar}{m}\vec{\nabla}\phi\right]|\psi|^2, \qquad [14]$$

with the phase ϕ defined by $\psi(r) = |\psi| e^{i\phi}$. If ϕ is constant, this is equivalent to the London equation, but the second term in [14] also leads to phenomena such as the Josephson effect.

The quantities λ and ξ_o are among the most important microscopic parameters. The ratio, $\kappa = \lambda/\xi_o$, divides Type-I and Type-II superconductors; those with $\kappa > 1/\sqrt{2}$ are Type-II superconductors, which exhibit magnetic vortices under the application of a magnetic field. On the other hand the Type I superconductors expel all magnetic fields, up to a critical field which causes the superconductor to become a normal metal.

Flux quantization comes naturally from the Ginzburg-Landau theory; integrating [14] about any closed loop deep within the superconductor (where $\vec{J}_{el}$ must be zero), and requiring the phase change to be 2π times an integer, one can obtain the quantization condition for the magnetic flux threading the loop ($\Phi = \int \vec{B}\cdot d\vec{s}$):

$$\Phi = \frac{hc}{2e} n \equiv \Phi_o n, \qquad [15]$$

with n an integer. The flux quantum is $\Phi_o = 2\times10^{-7}\,\mathrm{G\cdot cm^2}$. The magnetic vortices in Type II superconductors each carry one flux quantum of magnetic flux.

6. Superconducting materials overview:

Roughly ½ of the elements exhibit superconductivity, though in some cases only under extremely high pressures. Most nonmagnetic metals are included, although it is interesting that

copper, silver, and gold, the best normal metal conductors, cannot be made superconducting even under high pressure. (The reason; electron-phonon coupling normally drives electron pairing in superconductors, but the interaction is weak in noble metals, also reducing phonon-driven resistivity.) Magnetic materials usually do not exhibit superconductivity, since for the most part magnetism and superconductivity are mutually exclusive -- the fact that large applied magnetic fields will destroy the superconducting state was already mentioned. Elementary superconductors tend to be type I, with some important ones listed in Table I. Hg, Sn, and Pb superconductors were discovered by Onnes roughly 100 years ago. Nb is sometimes used for microfabricated SQUID sensors such as for magnetometers; it is also type II, as are a few other isolated elements.

Table I: Well-known elemental superconductors. All except Nb are type-I.

Element	T_c (K)	H_c (T)
Gallium (Ga)	1.1	0.005
Aluminum (Al)	1.2	0.01
Indium (In)	3.4	0.03
Tin (Sn)	3.7	0.03
Mercury (Hg)	4.2	0.04
Lead (Pb)	7.2	0.08
Niobium (Nb)	9.3	0.82

Alloys and compounds are generally type-II. Because of the much higher critical fields, superconductors for high-current applications such as magnets and power transformers are exclusively type II. A brief list of "non-high T_c" type II superconductors is in Table II. Among these $PbMo_6S_8$ is a Chevrel phase material; these attracted interest in the 1980s (pre-high T_c) as potential high-current superconductors because of their tolerance for magnetism, and related materials substituted with rare earth atoms have magnetism coexisting with superconductivity, in significant contrast to most superconductors in which just a few percent substitution of magnetic atoms destroys the superconducting state. UPt_3 and $CeCoIn_5$ are heavy Fermion superconductors: superconductivity grows out of a band of strongly-interacting Kondo-resonance states, and the magnetic excitations appear to be a fundamental part of the superconducting state [1], in contrast to BCS superconductors in which phonons drive the electron pairing.

Table II: Brief list of non-high-T_c superconducting compounds and materials.

compound	T_c (K)	compound	T_c (K)
Nb_3Sn	18	MgB_2	39
Nb_3Ge	23	$PbMo_6S_8$	15
NbN	16	UPt_3	0.48
$Nb_{0.6}Ti_{0.4}$	9.8	$CeCoIn_5$	2.3
carbon nanotubes	~15	Cs_2RbC_{60}	33

The materials on the left in table II include Nb alloys commonly used for high-current applications. Nb-Ti wires have excellent strength and current carrying capability, and are well established for magnet use. For higher current and field Nb_3Sn is often used—it is brittle and requires a reaction heat treatment after winding the magnet, but the technique is now well established. The picture at the left is a Nb-Ti wire (CERN website) with 6300 strands of 6 μm-dia. superconductor drawn within a copper matrix. This is typical configuration for magnet wire; the small filament diameter minimizes the motion of magnetic vortices, since dissipative vortex

motion is normally the limiting feature for current-carrying ability in such wires. Also shown (center) is a schematic of the "second generation" tape configuration developed for high-*Tc* cables.

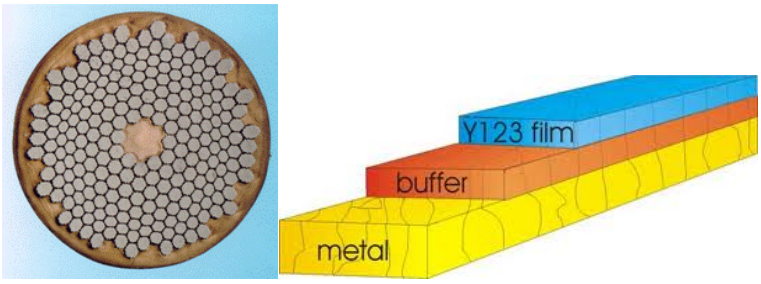

Among others in Table II, MgB_2 was discovered after the high-T_c cuprates and commanded attention as a simple and inexpensive compound with elevated T_c for power applications [2], though interest has been supplanted by the success with high-current cables made of high-T_c cuprates. Recent studies showing superconductivity in some configurations of carbon nanotubes [3] has attracted interest for making nano-devices. It has also been known for some time that doped buckyball (carbon fullerene) materials can exhibit superconductivity; the highest reported T_c is 33 K for Cs_2RbC_{60} [4]. There are also several well-established organic superconducting compounds that are of continued interest; generally the organic superconductors exhibit a variety of unconventional superconductivity and physically interesting behavior [5].

6. High-*Tc* superconductors and iron pnictides: "High-T_c" typically refers specifically to the cuprates, or copper-oxide superconducting materials. The first discovered was $La_{2-x}Sr_xCuO_4$, T_c = 38 K, by Bednorz and Müller in 1986 (Nobel prize 1987). There has since been a large number of copper-oxide-based superconducting compounds synthesized, including rare-earth-doped materials in which magnetism coexists with superconductivity. Table III, including some of the more important ones, is the same as what we saw earlier in class.

Table III: High-Tc cuprates, Fe pnictides, and related superconducting materials.

Compound	T_c (K)	Compound	T_c (K)
$(La,Sr)_2CuO_{4-\delta}$ (LSCO)	38	$LaFeAs[O_{1-x}F_x]$	26
$YBa_2Cu_3O_{7-\delta}$ (YBCO)	95	$GdFeAsO_{1-x}$	53
$Bi_2Sr_2CaCu_2O_9$ (BSCCO 2212)	110	$BaFe_2As_2$	38
$Bi_2Sr_2Ca_2Cu_3O_{10}$ (BSCCO 2223)	110	FeSe	8.5
$Hg_2Sr_2Ca_2Cu_3O_8$	134	LiFeAs	18
$(Nd,Ce)_2CuO_4$ (electron doped)	35	Sr_2RuO_4	0.93

$YBa_2Cu_3O_{7-\delta}$ (YBCO) was discovered by Paul Chu shortly after the initial discovery of $(La,Ba)_2CuO_{4-\delta}$. YBCO is technologically much more important with T_c above 77 K (nitrogen boiling point). The most widespread application for cuprate superconductors to date has been coils for high-efficiency microwave filters, ubiquitous in cell-phone towers. Bismuth-containing BSCCO has also become commercially important since the development of practical high-current cables. For power transmission-lines the technology is still not completely mature, though there have been a number of demonstration projects for power-grid and wind-generator applications.

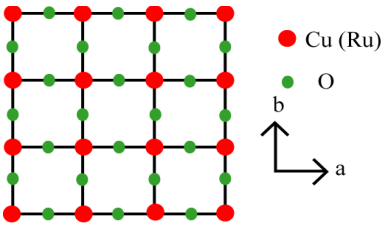

Structurally, the cuprates have planes containing (CuO_2) units, illustrated at left (Ru refers to the ruthenates [6], where the planes are composed of RuO.). Below is the full structure [6]: labeling is for $(La,Ba)_2CuO_{4-\delta}$ on the right, and $(Sr)_2RuO_{4-\delta}$ on the left. The cuprates fall into the general category of "perovskite"-structure materials, and there are many variations in the layered-structures, with for example larger unit cells containing more complicated sequences of *a-b* plane layers, as compared to the illustration.

In the formula $(La,Ba)_2CuO_{4-\delta}$, δ indicates missing oxygen ions between planes, creating holes; without them La_2CuO_4 is an insulating antiferromagnet. While most cuprates are hole doped, a few [such as $(Nd,Ce)_2CuO_4$ given in Table III] conduct through the addition of electrons. A schematic phase diagram for LSCO in the 3rd figure [7] shows how T_c exhibits a peak vs hole doping in the region where magnetic order disappears. This "superconducting dome" behavior has come to be recognized as a generic feature of unconventional superconductors [8], including heavy-Fermions and the iron pnictides. The prevailing view is that a zero-temperature phase transition, or "quantum critical point," lies below the dome, and fluctuations related to the phase transition drive the superconducting state.

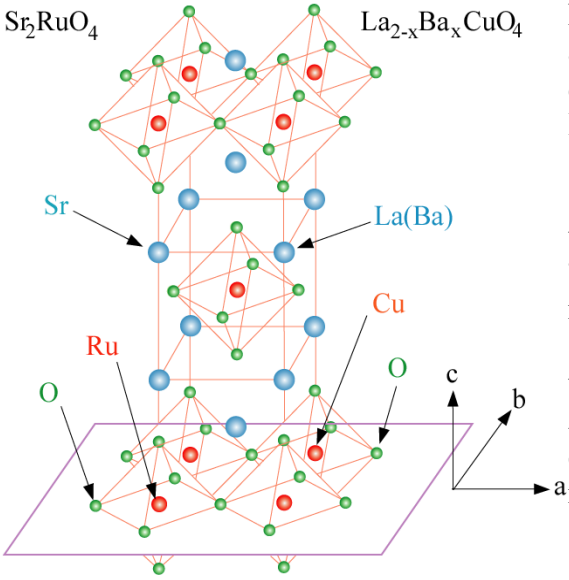

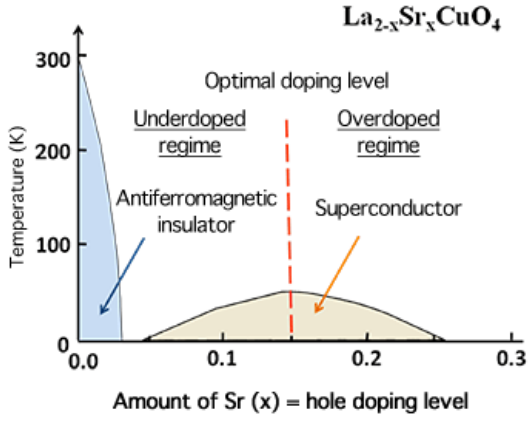

An additional feature of the cuprates is that they are electronically two-dimensional (more or less). From a band perspective, masses are very large in the *c* direction. Superconductivity thus is often modeled as parallel 2D superconducting sheets (the Cu-O planes) separated by insulating spacers, where superconducting pairs can move in the *c* direction only by tunneling. (Tunneling of superconducting pairs, as opposed to single electrons, is called Josephson tunneling.) This also can cause magnetic vortices in each layer to become decoupled, making the problem of flux pinning in high current wires more difficult [9].

The parameter $\kappa = \lambda / \xi_o$ is particularly large in the cuprates. For example in YBCO, λ and ξ are 100 nm and ~1 nm respectively, giving $\kappa = 100$. (ξ is even smaller in the *c* direction, perpendicular to the planes.) For comparison in aluminum $\lambda = 20$ nm and $\xi = 1000$ nm. ξ varies much more than λ between materials since it is related to the pair binding energy. ξ in cuprates is less than the spacing between Cu-O planes, implying pairs confined to one plane. This is the sense in which the superconductivity is 2-dimensional, with planes weakly coupled by tunneling.

Most cuprates as well as normal superconductors have pairs in which electrons have opposite spin. On the other hand, in Sr_2RuO_4 there is convincing evidence that pairs are in spin-triplet states [6]. Besides the general interest in such a situation, the spin-aligned state also implies the possibility for magnetic-field-tolerating superconductors useful for high-field magnets, with *B* fields less likely to break pairs if they are already magnetized. Note also that very recently triplet superconductivity has been of interest due to the potential for Majorana Fermion states, a hot topic in physics related to topological insulators as a new and interesting behavior. Majorana Fermions exist as their own antiparticles, with exchange symmetry much more complex than that of ordinary Fermions. Refer to reference [10] for more information.

Finally, the iron pnictide superconductors [11] are included in the right-hand column of Table III. The initial 2008 report of $La[O_{1-x}F_x]FeAs$ with surprisingly high T_c led to great interest in these materials that continues to the present. Magnetic-doped 1111 materials such as $GdFeAsO_{1-x}$ with higher T_c soon followed, and since then the 122 family ($BaFe_2As_2$), 111 (LiFeAs) and 11 FeSe and FeTe have been demonstrated as superconductors. These materials feature two-dimensional Fe-containing structural layers, and the picture that has emerged is unconventional superconductivity sharing many common features with the cuprates.

References:

[1] Magnetically mediated superconductivity in heavy fermion compounds, N. D. Mathur et al., Nature 394, 39 (1998), and many citations of this work.

[2] Superconductivity at 39 K in magnesium diboride, J. Nagamatsu et al., Nature 410, 63 (2001).

[3] Superconductivity in 4 Angstrom Single-Walled Carbon Nanotubes, Z. K. Tang et al., Science 292, 2462-2465 (2001).

[4] Superconductivity at 33 K in $Cs_xRb_yC_{60}$, K. Tanigaki, et al., Nature 352, 222 - 223 (1991); also see Superconductivity in a single-C_{60} transistor, C. B. Winkelmann et al., Nature Physics 5, 876 - 879 (2009).

[5] For a recent review see "Recent Topics of Organic Superconductors", A. Ardavan et al., J. Phys. Soc. Jpn. 81, 011004 (2012).

[6] Physics Today, Jan. 2001; Yoshiteru Maeno, T. Maurice Rice, and Manfred Sigrist, "T*he Intriguing Superconductivity of Strontium Ruthenate*."; Evaluation of Spin-Triplet Superconductivity in Sr_2RuO_4, Y. Maeno et al., J. Phys. Soc. Jpn. 81 (2012) 011009.

[7] "Imaging Doped Holes in a Cuprate Superconductor with High-Resolution Compton Scattering", Y. Sakurai, et al., Science 332, 698-702 (2011).

[8] See for example "What lies beneath the dome?", D. M. Broun, Nature Phys. 4, 170–172 (2008), part of Quantum Phase Transitions focus issue, Nature Phys. 4, 167-204 (2008).

[9] "Vortex physics in high-temperature superconductors," G. W. Crabtree and D. R. Nelson Physics Today, Apr. 1997.

[10] For an extended review, "New directions in the pursuit of Majorana fermions in solid state systems", J. Alicea, Rep. Prog. Phys. 75. 076501 (2012). See also "Introduction to topological superconductivity and Majorana fermions", M. Leijnse and K Flensberg, Semicond. Sci. Technol. 27 124003 (2012).

[11] Iron-based superconductors: Magnetism, superconductivity, and electronic structure (Review Article); A. A. Kordyuk, Low Temp. Phys. 38, 888 (2012); "Trend: High-temperature superconductivity in the iron pnictides", M. R. Norman, Physics 1, 21 (2008).

[12] Iron-Based Layered Superconductor $La[O_{1-x}F_x]FeAs$ ($x = 0.05-0.12$) with $T_c = 26$ K, Y. Kamihara et al., J. Am. Chem. Soc., 130, 3296–3297 (2008).